



1 **Volatile organic compounds and their role in secondary aerosol chemistry in a cold and dark**  
2 **urban environment**

3 James R. Campbell<sup>1</sup>, Brice Temime-Roussel<sup>2</sup>, Barbara D'Anna<sup>2</sup>, Kathy S. Law<sup>3</sup>, Weihang  
4 Zhang<sup>3</sup>, Rodney J. Weber<sup>4</sup>, Michael Battaglia Jr.<sup>4,†</sup>, Kayane K. Dingilian<sup>4,‡</sup>, Meeta Cesler-  
5 Maloney<sup>1</sup>, Jason M. St. Clair<sup>5,6</sup>, Jingqiu Mao<sup>1</sup>

6  
7 <sup>1</sup>Geophysical Institute and Department of Chemistry and Biochemistry, University of Alaska  
8 Fairbanks, Fairbanks, Alaska 99775, United States

9 <sup>2</sup>Aix Marseille Univ, CNRS, LCE, Marseille, France

10 <sup>3</sup>LATMOS/IPSL, Sorbonne Université, UVSQ, CNRS, Paris, France

11 <sup>4</sup>School of Earth and Atmospheric Sciences, Georgia Institute of Technology, Atlanta, Georgia  
12 30332, United States

13 <sup>5</sup>Atmospheric Chemistry and Dynamics Laboratory, NASA Goddard Space Flight Center,  
14 Greenbelt, Maryland 20771, United States

15 <sup>6</sup>Joint Center for Earth Systems Technology, University of Maryland Baltimore County,  
16 Baltimore, Maryland 21228, United States

17 <sup>†</sup>Present address: U.S. Army DEVCOM CBC, Aberdeen Proving Ground, Maryland, USA

18 <sup>‡</sup>Present address: Division of Chemistry and Chemical Engineering, California Institute of  
19 Technology

20 *Correspondence to:* James R. Campbell ([jrcampbell6@alaska.edu](mailto:jrcampbell6@alaska.edu))

21

22 **Abstract.** The role of volatile organic compound (VOC) emissions in secondary aerosol chemistry  
23 in urban subarctic environments remains poorly understood. Previous studies in wintertime  
24 Fairbanks, Alaska suggest that aldehydes may serve as precursors of S(IV) species in aerosols,  
25 contributing to the high concentrations of wintertime PM<sub>2.5</sub> pollution that Fairbanks often  
26 experiences. It is not known to what extent VOCs participate in secondary aerosol chemistry, or  
27 what the sources of largely secondary VOCs (like formaldehyde) are in such a cold and dark  
28 environment. Here, we explore the sources of VOCs and examine their role in secondary chemistry.  
29 We use measurements from an online proton transfer reaction time of flight mass spectrometer  
30 (PTR-ToF-MS), combined with complementary gas and aerosol measurements from the the  
31 Alaskan Layered Pollution and Chemical Analysis (ALPACA) wintertime field campaign in 2022,



32 to examine VOC sources and their roles in aerosol chemistry in downtown Fairbanks. We find that  
33 alcohols, aromatics and carbonyls together account for ~70% of measured VOCs, with methanol,  
34 ethanol, formaldehyde, benzene and toluene as dominant species. Positive matrix factorization  
35 (PMF) analysis indicates that approximately 56% of VOCs are associated with vehicle emissions,  
36 while wood heating and heating oil together contribute about 14%. Formaldehyde is primarily  
37 linked to diesel emissions, as well as primary and secondary sources associated with aged air  
38 masses. By comparing PMF factors with measured PM<sub>2.5</sub> S(IV) species, we find that vehicle-  
39 related emissions of ammonia and formaldehyde likely play a key role in the formation of  
40 hydroxymethanesulfonate (HMS) in Fairbanks.

41

## 42 **1 Introduction**

43 Volatile organic compounds (VOCs) are associated with many serious adverse health  
44 effects (Sharma et al., 2018; Zhou et al., 2025). While the majority of VOCs are of biogenic origin  
45 on a global scale (Guenther et al., 1995), anthropogenic sources can dominate in urban  
46 environments. VOCs can undergo secondary processes, typically via photooxidation. This can lead  
47 to the formation of secondary products like fine particulate matter and ozone (Grosjean et al., 1983;  
48 Seinfeld and Pandis, 2016; Ziemann and Atkinson, 2012), which have been further associated with  
49 adverse health effects (Nuvolone et al., 2018; Pope III and Dockery, 2006; Schwartz et al., 2002).

50 Fairbanks, Alaska is a subarctic town which often experiences episodes of poor air quality.  
51 The Fairbanks North Star Borough frequently violates the EPA PM<sub>2.5</sub> (particles with an  
52 aerodynamic diameter of < 2.5 μm) air quality standard of 35 μg/m<sup>3</sup> in the wintertime, exacerbated  
53 by strong inversion layers limiting dispersion (Cesler-Maloney et al., 2022; Simpson et al., 2024).  
54 Previous work has shown increased hospitalizations for cerebrovascular disease and respiratory  
55 tract infections in Fairbanks during periods of high PM<sub>2.5</sub> pollution (Kossover, 2010).

56 Despite a focus on achieving reductions in PM<sub>2.5</sub> (Campbell et al., 2022; Kotchenruther,  
57 2016; Nattinger, 2016; Ward et al., 2012), VOCs in Fairbanks have received less attention.  
58 Wintertime Fairbanks is unique as an urban environment, with temperatures down to -40 °C and  
59 only a few hours of daylight. Under these conditions biogenic VOC emissions are insignificant,  
60 and secondary VOC production related to UV photooxidation is expected to be small. Dark aging



61 of VOCs may be taking place, although to what extent is not clear. Many VOCs have an  
62 appreciable decrease in volatility in such cold temperatures, leading to more organic aerosol mass  
63 than predicted (Ijaz et al., 2025). Analysis shows that levels of hazardous VOCs like benzene,  
64 toluene, and C8 aromatics (ethylbenzene, xylene) can be up to ten times higher in Fairbanks  
65 compared to other US wintertime cities (Ketcherside et al., 2025; Simpson et al., 2024).

66 Certain VOC species can also form organosulfur compounds in the aerosol phase, such as  
67 hydroxymethanesulfonate (HMS) (Boyce and Hoffmann, 1984). In downtown Fairbanks, elevated  
68 mixing ratios of formaldehyde—comparable to wintertime levels observed in the North China  
69 Plain (Campbell et al., 2022; Song et al., 2019)—were found to play a key role in the formation of  
70 HMS. Acetaldehyde and other carbonyls can also form similar S(IV) adducts, leading to higher  
71 aerosol S(IV) concentrations (Dingilian et al., 2024; Holen et al., 2025). HMS and other S(IV)  
72 species account for a significant fraction of PM<sub>2.5</sub> mass in Fairbanks, particularly when compared  
73 to measurements in other urban environments (Campbell et al., 2022, 2024). The sources of  
74 formaldehyde and other aldehydes in Fairbanks remain poorly characterized, limiting our  
75 capability of developing mitigation strategies.

76 Positive matrix factorization (PMF) has been used extensively to quantify sources of VOCs  
77 in urban settings (Baudic et al., 2016; Gkatzelis et al., 2021; Huang et al., 2024; Ketcherside et al.,  
78 2025; McDonald et al., 2018; Rivellini et al., 2024; Sadeghi et al., 2022). Some studies done in the  
79 US have reported that the fraction of pollution related to vehicle emissions have decreased, and  
80 volatile chemical products (VCPs) from consumer and industrial products have become the  
81 dominant source of urban VOCs (Gkatzelis et al., 2021; McDonald et al., 2018). It is not clear  
82 whether this trend of decreasing vehicle emissions holds true for Fairbanks; many studies have  
83 found that certain VOC emissions can be more than an order of magnitude higher for both gasoline  
84 and diesel vehicles when cold-starting at -7 °C compared to 23-24 °C (Cao et al., 2024; Ferrarese  
85 et al., 2024; George et al., 2015; Hays et al., 2017; Liu et al., 2023). However, Fairbanks commonly  
86 experiences temperatures down to -40 °C and, unlike many places, Alaska does not use ethanol-  
87 blended fuels. We are not aware of any work that has examined vehicle emissions at temperatures  
88 as low as Fairbanks, nor that uses non-ethanol-blended fuel, so it remains unclear how prominent  
89 vehicle VOC emissions are in Fairbanks.



90 Several studies have conducted PMF analysis for gas and aerosol measurements during  
91 ALPACA field campaign. Ketcherside et al. (2025) combined PTR-ToF-MS VOCs, PM<sub>2.5</sub>, and  
92 gaseous measurements of SO<sub>2</sub>, CO, ozone, and NO<sub>x</sub> to examine sources of gases and aerosols in  
93 a residential neighborhood. They find that aromatic VOCs make up 50% of the total VOC mixing  
94 ratio, and are mainly attributed to traffic. Formaldehyde was found to come from various sources,  
95 and many other VOCs were mainly attributed to residential wood combustion. As the VOC  
96 measurements in their work were conducted 3 km away from downtown Fairbanks in a residential  
97 area, their analysis is likely more influenced by residential factors such as space heating. Ijaz et al.  
98 (2024) used downtown PM<sub>1</sub> measurements from both a PTR-ToF-MS with a CHARON inlet and  
99 an AMS to conduct PMF. They found that most PM<sub>1</sub> OA was attributed to residential heating when  
100 using the CHARON PTR-ToF-MS measurements. However, the role of VOCs in secondary  
101 aerosol chemistry has not been addressed in these studies.

102 Here, we analyze VOC measurements from an online PTR-MS in downtown Fairbanks  
103 and use PMF to identify VOC sources during the ALPACA campaign in 2022. We also discuss  
104 our PMF solutions with Ketcherside et al. (2025) to highlight the differences and similarities  
105 between the downtown site and the House site. To our knowledge this is the first study to have  
106 two sets of PTR-MS measurements under the same airshed. We further compare our PMF solutions  
107 with complementary gas and aerosol measurements to identify main drivers for formation of S(IV)  
108 species in aerosols in Fairbanks.

109

## 110 **2 Methods**

### 111 **2.1 Measurements**

112 Measurements were conducted in a trailer in downtown Fairbanks next to the University  
113 of Alaska Fairbanks Community and Technical College (64.84064°N, 147.72677°W, elevation  
114 136 m above sea level) from 17 January to 25 February 2022 as part of the 2022 ALPACA  
115 campaign, unless stated otherwise. Detailed information about the ALPACA campaign can be  
116 found in Simpson et al. (2024).

117 A proton-transfer-reaction time-of-flight mass spectrometry (PTR-TOF 6000 X2, Ionicon  
118 Analytik GmbH, Austria) was used to monitor VOC for 15 minutes at 20-second intervals, each



119 hour. The instrument was operated at a low E/N of 65 Td (i.e., drift voltage/pressure; pressure,  
120 temperature, and voltage of the drift tube were set at 2.6 mbar, 120°C, and 230 V) and in RF mode  
121 for optimal sensitivity. Raw PTR-ToF-MS spectra were processed with the commercial Ionicon  
122 Data Analyzer (IDA) software to fit high-resolution mass peaks and extract the corresponding time  
123 series. Times series were post-processed (i.e., background subtraction, conversion of raw signal to  
124 mixing ratios, 2-minutes temporal averaging, PMF input generation) with an in-house data  
125 processing tool, PeTeR Toolkit (version 6.0; Igor 6.37).

126 Mixing ratios were calculated using Eq. (1):

$$127 \quad R = \frac{RH^+}{H_3O^+} \times \frac{Tr_{H_3O^+}}{Tr_{RH^+}} \times \frac{U_{drift} \times T_{drift}^2}{k \times \tau \times p_{drift}^2} \quad (1)$$

128 Where  $RH^+$  and  $H_3O^+$  are the signal intensities in counts per second (cps) of the individual  
129 protonated ion and the reagent ion corrected by their relative transmission ( $Tr$ ) respectively,  $U_{drift}$ ,  
130  $T_{drift}$ ,  $p_{drift}$  and  $\tau$  are the voltage (V), temperature (K), and pressure (mbar) residence time (s) of the  
131 ions in the drift tube respectively,  $k$  the reaction rate ( $\text{cm}^3 \cdot \text{s}^{-1}$ ) between the reagent ion and VOC.

132 A 12-component mix at ppmV level (Apel Riemer Environmental Inc, Miami, USA) in the  
133 range of 32–134 amu diluted in pure nitrogen was used to experimentally determine the relative  
134 ion transmission at the beginning and at the end of the measurement campaign.

135 Compound-specific proton-transfer reaction rate constants ( $k$ ) were applied for VOCs  
136 where available in the literature (Cappellin et al., 2012). For all other species, a rate constant of  $2$   
137  $\times 10^{-9} \text{ cm}^3 \text{ s}^{-1}$  was assumed; this is a common value used when a measured rate constant is  
138 unavailable (Cappellin et al., 2012; Wang et al., 2020, 2021). An additional correction was applied  
139 to ethanol using calibration coefficients obtained from post-campaign laboratory measurements,  
140 as significant fragmentation resulted in an underestimation of ethanol mixing ratios by a factor of  
141 9 when default reaction rate constants were assumed.

142 Alongside the PTR-ToF-MS, two additional formaldehyde measurements were made using  
143 a MIRA Ultra Gas Analyzer (Aeris Technologies) and COmpact Formaldehyde Fluorescence  
144 Experiment (COFFEE) (St. Clair et al., 2017). Correlations between all three instruments were  
145 high ( $r^2$  ranging from 0.69 and 0.81, Fig. S1) but the PTR-ToF-MS measurements were about four  
146 times lower than both the MIRA Ultra Gas Analyzer and COFFEE. This is because formaldehyde



147 has a proton affinity close to water, so the back reaction of protonated formaldehyde with water  
148 vapor becomes relevant and reduces the sensitivity of formaldehyde in the PTR-ToF-MS  
149 (Vlasenko et al., 2010). Therefore, the formaldehyde measured by the PTR-ToF-MS was scaled  
150 up to match these instruments. Mixing ratios were corrected for background contribution using a  
151 cylinder of high purity nitrogen (99.999 purity).

152 Other non-VOC measurements made at the CTC site were used for comparison with the  
153 PMF results. PM<sub>1</sub> OA, sulfate, nitrate, and ammonium were measured by an Aerosol Mass  
154 Spectrometer (AMS). Black Carbon (BC) was measured by a Multi-Angle Absorption Photometer  
155 (MAAPS). Other CTC measurements include carbon monoxide (CO), SO<sub>2</sub>, NO<sub>x</sub>, ozone (O<sub>3</sub>),  
156 temperature, wind speed and wind direction. Total ammonium was measured using a mist chamber  
157 coupled with ion chromatography (MC-IC) (Cofer et al., 1985), and total S(IV) was measured  
158 using a particle into liquid sampler coupled with ion chromatography (PILS-IC) (Orsini et al.,  
159 2003). Both MC-IC and PILS-IC methods have been discussed in other ALPACA papers  
160 (Campbell et al., 2024; Dingilian et al., 2024; Simpson et al., 2024).

161 The PTR-ToF-MS is unable to detect short-chain alkanes with less than C<sub>8</sub> such as ethane,  
162 propane, and butane due to their low proton affinities. Very few works contain a comprehensive  
163 overview of both oxygenated VOCs and short-chain alkane VOCs in the US. The CalNex  
164 campaign, which used multiple instruments to measure both categories as described in Heald et al.  
165 (2020), found that short-chain alkanes made up on average 36.5% of the total measured  $\mu\text{gCsm}^{-3}$ ,  
166 excluding organic aerosols. Heald et al. (2008) contains VOC measurements from other North  
167 American campaigns, although not all VOCs were measured for all campaigns. Ethane, propane,  
168 and butane range from 7.5-37.2% of the measured  $\mu\text{gCsm}^{-3}$  for measurements done in the US and  
169 Canada, excluding organic aerosols. A direct comparison between these works and Fairbanks are  
170 difficult due to the unique climate of Fairbanks, but we expect short-chain alkanes and alkenes to  
171 be in a similar range.

## 172 **2.2 Positive Matrix Factorization (PMF)**

173 PMF is a mathematical model commonly used to estimate source contributions of VOCs  
174 datasets. Briefly, the PMF model uses a time series dataset matrix and corresponding error matrix  
175 as inputs. The user specifies a number of factors—in our case, the number of factors equates to the  
176 number of VOC sources. The PMF model attempts to split the main dataset into two matrices: a



177 time series of factors, and the contribution of each VOC species to each factor. The user then  
178 interprets the resulting matrices to determine what source each factor corresponds to. More  
179 detailed information about the model can be found in literature (Paatero, 1999). We used SoFi Pro  
180 version 9 which utilizes the ME-2 engine (Canonaco et al., 2013; Paatero, 1999). Over 300 ions  
181 were included for PMF analysis. An error matrix was also calculated with the PeTeR tool by  
182 propagating uncertainties in ion counts and background signals, assuming Poisson counting  
183 statistics (de Gouw and Warneke, 2007). The data was down-weighted based on the  
184 recommendations of Paatero and Hopke (2003).

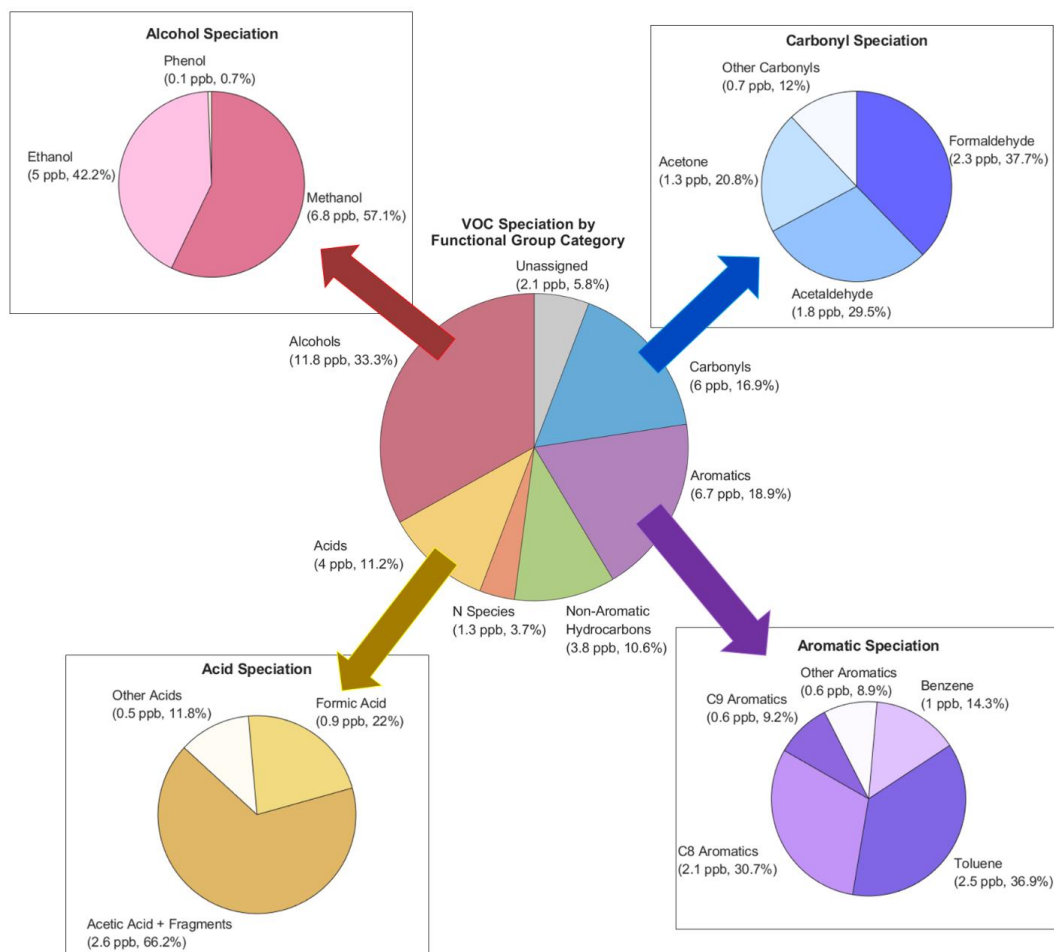
185

### 186 **3 Results and Discussion**

#### 187 **3.1 Overview of VOC Measurements in Downtown Wintertime Fairbanks**

188 We first examine the campaign average for VOC measurements. The mean VOC mixing  
189 ratio during the campaign was 35.6 ppb. Here, for simplicity, we describe VOC composition for  
190 species which had a campaign average of 0.05 ppb or higher. This included 46 species which  
191 account for 33.6 ppb (94.3% of the total VOC mixing ratio). It should be noted that there were two  
192 periods of enhanced pollution during the ALPACA campaign, as described in Simpson et al.  
193 (2024). Figure S2 shows  $PM_{10}$  (measured by aerosol mass spectrometer, described below) and  
194 temperature during the campaign, with the pollution events highlighted.

195 Figure 1 shows the percent contributions and campaign-mean VOC mixing ratios by  
196 functional group (see Table S1 for details). Alcohols, aromatics, carbonyls, acids, non-aromatic  
197 hydrocarbons, and nitrogen-containing species are the dominant VOC classes. Alcohols were by  
198 far the most prominent category due to the high mixing ratio of methanol (6.8 ppb) and ethanol (5  
199 ppb) during the campaign. The species with the third largest mean mixing ratio was formaldehyde  
200 at 2.3 ppb. Common species from other functional group categories are (in decreasing order):  
201 toluene, C8 aromatics, benzene, and C9 aromatics for aromatics; formaldehyde, acetaldehyde and  
202 acetone for carbonyls;  $C_2H_4O_2$  (acetic acid) and formic acid for acids. The speciation is similar  
203 with median values (Fig. S3).



204

205 Figure 1. Mean composition of VOCs categorized by their functional groups during ALPACA  
 206 campaign. The “Unassigned” group is made of up of about 290 species whose individual campaign  
 207 means are all less than 0.05 ppb.

208

209 Methanol and ethanol are highest from Jan 21<sup>st</sup> to Jan 25<sup>th</sup> before the first pollution event,  
 210 with methanol spikes up to 166 ppb and ethanol spikes up to 180 ppb. Interestingly, as shown in  
 211 Table S2 and Fig. S4a, there was not much enhancement of methanol and ethanol during the cold  
 212 polluted event compared to periods outside the pollution events, but they were significantly



213 increased during the warm pollution event, with methanol spikes up to 133 ppb. Both are similar  
214 mixing ratios to measurements at the house site in Ketcherside et al. (2025).

215 The methanol in wintertime Fairbanks is on average 1.2-2 times higher than other urban  
216 wintertime measurements in the US and China (Li et al., 2019; Millet et al., 2005), and 2-6 times  
217 higher than measurements in Europe (Languille et al., 2020; Legreid et al., 2007; Patokoski et al.,  
218 2014). The large discrepancy of methanol between Fairbanks and Europe may be because the US  
219 and Canada use methanol-based windshield wiper fluid and Europe uses ethanol-based. Legreid  
220 et al. (2007) attributes the high ethanol mixing ratios in Zürich, Switzerland to windshield wiper  
221 fluid. Slowik et al. (2010) attributes high levels of methanol due to windshield wiper fluid in  
222 Toronto, Canada, but did not report a mixing ratio. We further discuss the influence of windshield  
223 wiper fluid in Fairbanks in Section 3.2. Ethanol in Fairbanks is between 1.2-5 times higher than  
224 measurements in the US and Europe (Gkatzelis et al., 2021; Legreid et al., 2007; Millet et al.,  
225 2005).

226 The aromatics were mainly made up of toluene (2.5 ppb) and C8 aromatics (xylenes and  
227 ethylbenzene, 2.1 ppb), benzene (1.00 ppb) and C9 aromatics (0.62 ppb). All species show  
228 enhancements during the polluted episodes, with similar mixing ratios during the cold and warm  
229 pollution events (Fig. S4b, Table S2). The mean aromatic mixing ratio in Ketcherside et al. (2025)  
230 is 11.9 ppb, almost double what is reported in this work. All aromatics are higher at the house site,  
231 with C8 aromatics having the largest discrepancy—nearly 3 times higher at the house site than  
232 downtown. This likely reflects a greater influence of heating oil combustion in residential areas.  
233 The mixing ratios of aromatics in this work are 2-12 times higher than those reported during other  
234 North American wintertime campaigns in urban locations like NYC, NY (Gkatzelis et al., 2021);  
235 Boulder, CO (Gkatzelis et al., 2021); Pittsburgh, PA (Millet et al., 2005); Houston, TX (Sadeghi  
236 et al., 2022); and Toronto, Canada (Rivellini et al., 2024). Benzene, toluene and C8 aromatic levels  
237 are comparable to urban and suburban wintertime measurements in China (Li et al., 2015, 2019).

238 The high aromatic mixing ratio in wintertime Fairbanks compared to other US cities is also  
239 likely due, in part, to differences in gasoline composition. Yano et al. (2016) measured the aromatic  
240 content of Anchorage, AK gasoline in 2013, after new gasoline regulations took place nationwide.  
241 They found benzene content was 1.3% v/v, and the total aromatic content (benzene, toluene,  
242 ethylbenzene, and xylene) was 25% v/v. This is more than double the average benzene content in



243 gasoline in 2013 (0.6% v/v), and about 1.3 times higher than the total aromatic content (19% v/v)  
244 provided by the United States Environmental Protection Agency  
245 (<https://nepis.epa.gov/Exe/ZyPDF.cgi?Dockey=P100T5J6.pdf>). The relatively high aromatic  
246 content in Alaskan gasoline, combined with increased vehicle emissions at cold temperatures,  
247 leads to high gas-phase aromatic mixing ratios.

248 The greatest carbonyl species was formaldehyde (2.3 ppb), followed by acetaldehyde (1.8  
249 ppb) and acetone (1.2 ppb). Nine other carbonyls had mean values between 0.05-0.17 ppb (Table  
250 S1). Formaldehyde, acetaldehyde and acetone are all enhanced during the pollution periods (Fig.  
251 S4c, Table S2). Formaldehyde is noticeably much higher during the cold event, whereas  
252 acetaldehyde is highest during the warm event. In contrast, measurements of formaldehyde (1.4  
253 ppb) and acetaldehyde (1.3 ppb) at the house site are on average 40-60% lower compared to  
254 downtown measurements. Acetone has a similar mixing ratio range to other wintertime  
255 measurements in the US, European, and China, although acetaldehyde is 2-3x higher (Gkatzelis et  
256 al., 2021; Legreid et al., 2007; Li et al., 2019; Millet et al., 2005). In another study, formaldehyde,  
257 acetaldehyde, and acetone are in a similar range to wintertime non-haze periods in Beijing, and  
258 about half as much when compared to haze periods (Rao et al., 2016).

259 Acetic acid (1.7 ppb) and formic acid (0.9 ppb) are the two most prominent acid species.  
260 Although these compounds often spike at the same time, in many periods formic acid increases  
261 while acetic acid decreases (Fig. S4d, see Jan 28-29, Feb 3-4, Feb 21-23), and they are poorly  
262 correlated (Fig. S5), suggesting that they are likely arising from different sources, instead of a  
263 shared source like wood heating. Acetic acid at the house site is lower (1.3 ppb) compared to the  
264 downtown site, but formic acid is similar. Formic acid is unique in that it is slightly lower during  
265 both pollution events compared to the clean periods (Table S2). This indicates a lack of primary  
266 sources of formic acid in downtown Fairbanks, and may be evidence of dark aging, which is  
267 discussed more in Section 3.2. Both formic acid and acetic acid are moderately lower than urban  
268 and suburban wintertime measurements in China (Li et al., 2019).

269 Mixing ratios of nonaromatic hydrocarbons and nitrogen species are generally low. The  
270 two most prominent nonaromatic hydrocarbon species are  $C_3H_6$  (1.7 ppb) and  $C_5H_8$  (0.4 ppb) (Fig.  
271 S6a), but these ions may also include fragmentation of larger VOCs (Coggon et al., 2024;  
272 Gueneron et al., 2015). Similarly, the most commonly measured nitrogen-containing ion was  $NO_2^+$



273 fragments (Fig. S6b), a common fragment for many organic nitrate species (Aoki et al., 2007;  
274 Hansel and Wisthaler, 2000).

275

### 276 **3.2 Nine Factor PMF Solution**

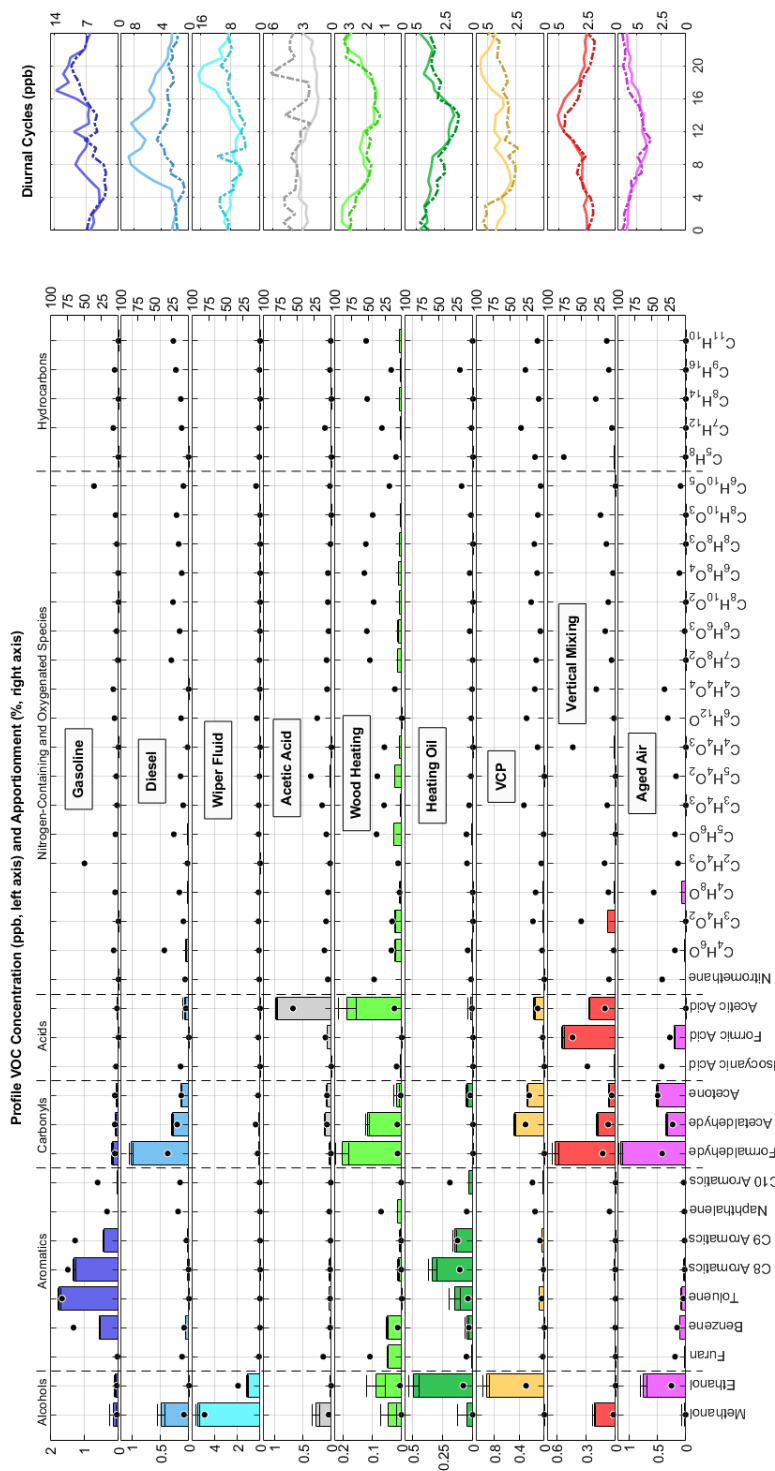
277 Nine factors were resolved from the PMF analysis. These factors are: gasoline, diesel,  
278 windshield wiper fluid, acetic acid, wood heating, heating oil, volatile chemical products (VCPs),  
279 vertical mixing, and aged air. Section S1 describes how VOC profiles, diurnal cycles, and  
280 correlation with external measurements were used to assign the PMF factors. A summary of the  
281 factors is shown in Fig. 2 and Table S3. A log-scale version of Fig. 2 is shown in Fig. S7, all  
282 species are shown in Fig. S8-S10, and time series of all factors is shown in Fig. S11. In the  
283 following, we define a VOC as negligible to a factor's composition when a VOC contributes less  
284 than 3% of its average campaign mixing ratio to a factor. The likely assignment of the VOC  
285 "C<sub>2</sub>H<sub>4</sub>O<sub>2</sub>" is acetic acid, however we refer to it by its chemical formula to avoid confusion with  
286 the acetic acid factor.

#### 287 **3.2.1 Traffic Factors: Gasoline and Diesel**

288 There are two traffic factors related to direct vehicle emissions—gasoline (6.4 ppb, 18.2%)  
289 and diesel (3.7 ppb, 10.6%). The gasoline factor is by far the largest source of aromatic species  
290 like benzene (65.8%), toluene (82.6%), C<sub>8</sub> aromatics (74.1%), and C<sub>9</sub> aromatics (63.4%). A little  
291 more than 5% each of formaldehyde, acetaldehyde, and acetone are explained by the gasoline  
292 factor. 6.9% of total benzene and 3.5% of total C<sub>9</sub> aromatics are associated with the diesel factor,  
293 but toluene and C<sub>8</sub> aromatics are negligible. The diesel factor is the largest primary source of  
294 formaldehyde, accounting for 30.8%; acetaldehyde and acetone are lower at 17.0% and 11.0%,  
295 respectively.

296 Both traffic factors are lower on weekends than during the weekdays, with diesel  
297 decreasing the most by nearly 50% (Fig. 2). This may indicate that heavy duty diesel vehicles that  
298 do not operate on weekends (school busses, public transportation, garbage trucks, etc.) account for  
299 much of the diesel emissions.

300



301

302 Figure 2. The left figures show the mixing ratio (left y-axis, ppb) and percent apportionment (right y-axis) of VOCs used to assign each  
 303 factor. The x-label shows either the chemical name for species which are likely to be dominated by one isomer, or the chemical formula  
 304 for species which are likely to have multiple isomers. The mixing ratio and percent for each species in each factor can be found in Tables  
 305 S7 and S8, respectively. The right figures show the weekday (solid line) and weekend (dashed line) mean diurnal cycles of the factors.



306           The gasoline and diesel factors do not have the same diurnal cycles, although this could be  
307 due to differences in cold start emissions between gasoline and diesel vehicles. The weekday and  
308 weekend diurnal cycles for each factor are shown in Fig. 2. The gasoline and diesel factors both  
309 increase early in the morning. Gasoline continues to increase until it peaks around 7 pm, whereas  
310 diesel starts to decrease around 2 pm. Since the site is downtown (as opposed to the residential  
311 areas outside of downtown), measurements in the morning will mainly be characterized by  
312 vehicles that have been started elsewhere and are driven into town, so the full impact of cold start  
313 emissions are not expected to be observed. After the typical workday is over, vehicles will be cold-  
314 started downtown, which would lead to an increase in gasoline vehicle emissions (Cao et al., 2024;  
315 George et al., 2015). However, diesel vehicle VOC emissions are less affected by cold starts  
316 overall compared to gasoline vehicles (Ferrarese et al., 2024; Marques et al., 2022; Wang et al.,  
317 2022), which leads to a much lower afternoon peak for diesel compared to gasoline. Some diesel  
318 vehicle emissions, especially carbonyls, can increase at low temperatures (Ferrarese et al., 2024;  
319 Hays et al., 2017; Liu et al., 2023; Suarez-Bertoa et al., 2022; Wærsted et al., 2022; Zhang et al.,  
320 2026), but to our knowledge emission measurements for VOCs diesel vehicles have not been  
321 carried out at the extremely low temperatures Fairbanks experiences.

### 322 **3.2.2 Other Vehicle-Related Factors: Windshield Wiper Fluid and Acetic Acid**

323           The windshield wiper fluid factor (7.2 ppb, 20.7%) is made up of 81.2% of the total  
324 measured methanol and 32.3% of the total ethanol. Contributions from other species are very small.  
325 The wiper fluid factor is the largest source of VOCs due to high mixing ratios of methanol  
326 measured during the campaign.

327           The acetic acid factor (2.4 ppb, 6.8%) may be related to vehicle emissions, as described in  
328 the SI. The acetic acid factor mainly consists of  $C_2H_4O_2$  (acetic acid), and 56.1% of the total  
329  $C_2H_4O_2$  measured is attributed to this factor. It does not have a well-defined diurnal cycle, as it is  
330 affected by large spikes of  $C_2H_4O_2$  which do not occur at regular intervals.

331           If the windshield wiper fluid and acetic acid factors are included with the gasoline and  
332 diesel factors, the total VOCs related to vehicles increases from 28.8% to 56.3%.

333

334



### 335 **3.2.3 Space Heating Factors: Wood Heating and Heating Oil**

336 Two factors were related to residential heating: wood heating (2.0 ppb, 5.6%) and heating  
337 oil (3.1 ppb, 8.8%). Although wood heating and heating oil are the largest and second largest  
338 contributors to PM<sub>2.5</sub> mass, respectively (Nattinger, 2016), their contribution to total VOC mixing  
339 ratios are relatively small at 14.2% total.

340 Residential wood heating is a moderate source of small carbonyl species, associated with  
341 6.2% of total formaldehyde and 6.7% of acetaldehyde. It is also associated with 5.9% of benzene,  
342 although other aromatics are negligible. Heating oil, which can be residential or commercial in  
343 downtown Fairbanks, is the second largest contributor to total aromatics, including 19.3% of C8  
344 aromatics and 22.6% of C9 aromatics. The wood heating factor is 6.1 times higher in the cold  
345 polluted period than the warm polluted period, a large increase in wood burning at these extremely  
346 cold temperatures.

347 Heating oil is associated with no formaldehyde or acetaldehyde, and 4.1% of the total  
348 acetone. The lack of formaldehyde assigned to the heating oil factor may be because heating oil  
349 boilers operate without after-treatment systems. In contrast, diesel vehicles can produce higher  
350 formaldehyde emissions due to oxidation of unburned fuel in their exhaust after-treatment systems,  
351 especially under cold conditions (Suarez-Bertoa et al., 2022).

### 352 **3.2.4 Volatile Chemical Products (VCP) Factor**

353 The VCP factor (3.1 ppb, 8.9%) is a minor contributor to VOCs in Fairbanks, in contrast  
354 to other US cities like LA, NYC, and Boulder, where it is becoming a main anthropogenic source  
355 of VOCs; McDonald et al. (2018) and Gkatzelis et al. (2021) find that the ratio of vehicle emissions  
356 to VCP emissions is between 0.3-1.4. In Fairbanks, we find that vehicle emissions are 3.2 times  
357 higher than VCPs when looking at only the combined gasoline and diesel factors, and 6.3 times  
358 higher when including the windshield wiper fluid and acetic acid factor. The relatively high  
359 contribution of VOCs related to vehicles is likely due to the increase in both gasoline and diesel  
360 vehicle VOC emissions at low temperatures (Cao et al., 2024; Ferrarese et al., 2024; George et al.,  
361 2015; Hays et al., 2017; Liu et al., 2023), and decreased volatility of VCPs at cold temperatures  
362 leading to less off-gassing. Overall, vehicle emissions remain the dominant source of VOCs in  
363 wintertime Fairbanks.



### 364 3.2.5 Vertical Mixing Factor

365 The vertical mixing factor (2.8 ppb, 7.9%) describes air masses that have been transported  
366 from outside downtown Fairbanks and have undergone secondary chemistry. 18.7% of total  
367 formaldehyde, 10.7% of acetaldehyde, and 5.5% of acetone are associated with the vertical mixing  
368 factor. Benzene, toluene, C8 aromatics and C9 aromatics are all negligible. This factor is the largest  
369 source of formic acid, accounting for 62.8%. The large fraction of formic acid, formaldehyde  
370 (18.7%), and maleic anhydride (64.3%), combined with the factor's correlation to ozone, may be  
371 indicative of secondary formation via ozonolysis and/or NO<sub>3</sub> radicals (Eliason et al., 2003; Li et  
372 al., 2023; Paulot et al., 2011). The vertical mixing factor explains much of the observed C<sub>3</sub>H<sub>4</sub>O<sub>2</sub>  
373 (50.3%), C<sub>2</sub>H<sub>4</sub>O<sub>3</sub> (16.1%), C<sub>3</sub>H<sub>4</sub>O<sub>3</sub> (75.6%), C<sub>4</sub>H<sub>4</sub>O<sub>3</sub> (62.5%), C<sub>5</sub>H<sub>6</sub>O<sub>3</sub> (28.9%), C<sub>4</sub>H<sub>4</sub>O<sub>4</sub> (28.2%),  
374 and C<sub>5</sub>H<sub>6</sub>O<sub>4</sub> (29.7%). These species are associated with aged residential biomass burning plumes  
375 (Coggon et al., 2019; Li et al., 2023) and decomposition of aromatic VOCs (Lannuque et al., 2023;  
376 Mehra et al., 2020). And, as mentioned earlier, formic acid mixing ratios are lower during both  
377 polluted events with strong surface inversions, indicating few primary sources of formic acid in  
378 downtown Fairbanks. As discussed in Brett et al. (Brett et al., 2025), residential space heating  
379 emissions are emitted above the surface. Thus, wood heating plumes may be transported aloft from  
380 areas with prominent wood heating emissions, during which longer chain VOC species are  
381 oxidized by ozone and/or NO<sub>3</sub> radicals, and break down into smaller chain VOCs, producing  
382 formaldehyde and especially formic acid. A similar OVOC<sub>Ox</sub> factor was observed in Wang et al.  
383 (2024). It had similarities to the time series of O<sub>3</sub>+NO<sub>2</sub>, contributions from low mass oxidized  
384 compounds like formic acid, and high contribution from C<sub>x</sub>H<sub>y</sub>O<sub>3</sub> ions, which they relate to  
385 daytime photochemistry.

386 We further evaluate the vertical mixing factor by comparing it and ozone to wind speed  
387 and direction. Ozone, as shown in Fig. S12, increases significantly when wind speed is greater  
388 than 3 mph. These higher wind speeds coincide with weakly stable periods and lower NO<sub>x</sub>, and  
389 more vertical mixing, as discussed in Brett et al. (2025). In contrast, strongly stable stagnant  
390 conditions correspond to low wind speeds, and are associated with high NO<sub>x</sub> which titrates ozone.  
391 At the surface, during periods of higher wind speeds, air masses mainly come from 0-100°  
392 (northeast to east direction) or 210-280° (southwest to west). However, as shown in Fig. S12, the  
393 vertical mixing factor (at the surface) only increases when wind directions are from the east (80-



394 100°). This shows that not only wind speed, but also the wind direction matters for the vertical  
395 mixing factor. Figure S13 show the high wind speed vectors overlaid on a map of Fairbanks, with  
396 points colored by the mixing ratio of the vertical mixing factor. We can see that periods associated  
397 with a higher mixing ratio come from Fort Wainwright and the northern part of the town Badger.  
398 It is also possible that plumes from the nearby town of North Pole, which has greater use of wood  
399 heating compared to Fairbanks (Nattinger, 2016), are included in these air masses. Higher wind  
400 speeds from less populated areas like Steele Creek and Ester have lower mixing ratios.

### 401 **3.2.6 Aged Air Factor**

402 The aged air factor (4.4 ppb, 12.6%) contains relatively stable products of atmospheric  
403 reactions involving a wide range of VOCs, and accounts for 21.2%, 34.7%, 19.4%, and 41.2% of  
404 the variability of ethanol, formaldehyde, acetaldehyde, and acetone, respectively. Notably, it is  
405 also the factor with the second largest amount of formic acid (23.5%), which we associate with  
406 secondary chemistry. It has a low contribution of markers of primary emissions, does not correlate  
407 well with any usual tracers or external measurements, and has small diurnal variability. This  
408 indicates that this factor is secondary in nature, representing the regional background. It has a low  
409 contribution from primary emission markers (12.7% of benzene and 3.7% of toluene is related to  
410 this factor, but other aromatics are negligible).

### 411 **3.2.7 Factor Summary**

412 According the PMF result, vehicle-related factors are the largest source of VOCs in  
413 downtown Fairbanks. Gasoline vehicles are by far the largest source of all major aromatic species  
414 like benzene, toluene, C8 aromatics, and C9 aromatics. A smaller but still significant fraction is  
415 attributed to heating oil, especially C8 (19.3%) and C9 aromatics (22.6%). Sources of carbonyl  
416 species are more variable. Diesel is the largest primary source of formaldehyde (30.8%). The  
417 vertical mixing and aged air factors account for about 53% of the formaldehyde, which may be a  
418 mixture of primary and secondary sources. The three largest sources of acetaldehyde are (in  
419 decreasing order) VCPs, aged air, and diesel. The three largest sources of acetone are (in  
420 decreasing order) aged air, VCPs, and diesel.

421

422



### 423 3.3 Comparison with Other PMF Work in Fairbanks

424 Ketcherside et al. (2025) also used PTR-ToF-MS data in Fairbanks to conduct PMF of  
425 VOC measurements in Fairbanks, but there are a few main differences. First, their instrumentation  
426 was located in a residential area 2.6 km away from the CTC site. Therefore, their analysis is likely  
427 more influenced by residential factors, like space heating. Second, in their PMF analysis they  
428 included species that were measured at the house site by instruments besides PTR-ToF-MS, like  
429 the gas-phase species CO and NO<sub>x</sub>, as well as aerosol-phase PM<sub>1</sub> species like BC, sulfate, nitrate,  
430 and ammonium. They also include SO<sub>2</sub> measured at the CTC site. In our analysis, we only use  
431 PTR-ToF-MS data as inputs for PMF analysis, but we do compare the PMF outputs to the  
432 corresponding CTC measurements of these species. Third, their analysis is based on hourly  
433 measurements, while ours is based on 2-minute data. They also use the EPA PMF 5.0 software  
434 while we use SoFi Pro V9; however, both are based on the ME-2 engine (Canonaco et al., 2013;  
435 Norris et al., 2014) so the PMF procedures should be largely similar. More information on the  
436 differences between these two sites and the instrumentation at the house site can be found in  
437 Simpson et al. (2024) and Ketcherside et al. (2025).

438 Despite the different methodology, there are many similarities between our work and the  
439 results in Ketcherside et al. (2025). Both studies found factors related to vertical mixing (which  
440 they call ozone), aged air, heating oil, wood heating (i.e., biomass burning), and traffic. Their study  
441 identifies two biomass burning factors (one for short-lived VOCs and one for long-lived), while  
442 we only have one. We find two traffic factors, while in their six factor solution they only find one.  
443 Their traffic diurnal cycle is most similar to our gasoline factor. We find the wiper fluid, VCP, and  
444 acetic acid factor, which they did not. They found that methanol was largely associated with traffic  
445 emissions, which is similar to our assignment of methanol to windshield wiper fluid. They also did  
446 not observe the large spikes of C<sub>2</sub>H<sub>4</sub>O<sub>2</sub> that we find, which helps to confirm that our analysis of  
447 C<sub>2</sub>H<sub>4</sub>O<sub>2</sub> are local to the CTC site. They mainly attribute C<sub>2</sub>H<sub>4</sub>O<sub>2</sub> and formic acid to biomass  
448 burning, while find that much of the C<sub>2</sub>H<sub>4</sub>O<sub>2</sub> is in its own factor, and formic acid is mainly  
449 attributed to the vertical mixing factor. Figure S14 presents pie charts of the PMF factor  
450 contributions from our work and Ketcherside et al. (2025) It is notable that wood heating and  
451 heating oil are a significantly smaller fraction in our work compared to theirs. Figure S15 can be  
452 used for further comparison of PMF factors with their Fig. S5.



453 Both our study and Ketcherside et al. (2025) find traffic to be the largest source and heating  
454 oil to be the second largest source of aromatic VOCs. However, in our results the gasoline factor  
455 dominates, making up 75% of the total benzene, toluene, C8 aromatics, and C9 aromatics, while  
456 heating oil only makes up 13%. In Ketcherside et al. (2025), gasoline makes up 48% and heating  
457 oil makes up 39%. This is large difference likely due to the increased influence of space heating  
458 at the residential site compared to the CTC site.

459 Ketcherside et al. (2025) attributes 18% of formaldehyde to heating oil, whereas we do not  
460 see any formaldehyde associated with heating oil. Here we describe some possible reasons for this  
461 discrepancy. This difference could be due to the different time resolution used in our works. The  
462 measurements in Ketcherside et al. (2025) were averaged to one hour, while our measurements are  
463 every two minutes. Heating oil and diesel fuel are compositionally similar but the combustion  
464 process is different, so the emissions are comparable but not identical. Our two-minute data may  
465 be able to resolve the differences between heating oil and diesel emissions more effectively.  
466 Another reason is that since their work was conducted at a residential site with less traffic than our  
467 CTC site, diesel emissions are expected to be much smaller and thus may be more difficult to  
468 distinguish from heating oil. Since the CTC site is much more dominated by traffic emissions, the  
469 variation of formaldehyde related to heating oil may be difficult to distinguish from other factors.  
470 Qualitatively, their heating oil factor contains characteristics of both our diesel and heating oil  
471 factors—for example, a 5 am increase similar to our diesel factor, and an afternoon increase present  
472 in our heating oil factor.

473 Our wood heating factor appears to be most comparable to the short-lived biomass burning  
474 factor in Ketcherside et al. (2025), including similarities between the furan, methylfuran, furfural,  
475 and methylfurfural assignments, and their diurnal cycles (Fig. 2, Table S4). Meanwhile, our  
476 vertical mixing factor has similarities to the chemical composition of their long-lived biomass  
477 burning factor (notably formic acid and formaldehyde, as well as furans and other aldehydes, Table  
478 S4) but the diurnal cycle of the vertical mixing factor is closer to their ozone factor (diurnal cycles).  
479 The discrepancy between chemical composition and diurnal cycles may be because 98% of ozone  
480 gas was applied to their ozone factor. Although our vertical mixing factor is correlated with ozone  
481 gas, there are also periods where ozone gas and the vertical mixing factor are not in agreement



482 (Fig. S12). Their ozone factor describes the transport of background levels of ozone from all wind  
483 directions, but our vertical mixing factor is highest when wind direction is from the east.

484 We cannot compare the source apportionment of species like CO, NO<sub>x</sub>, BC, and PM<sub>1</sub>  
485 sulfate because we used these species as external validation to compare with the PMF results.  
486 However, we do find that CO, NO<sub>x</sub>, and BC are well-correlated with traffic (Fig. S16 and S17),  
487 which is consistent with these species being associated with their traffic factors.

488 Ijaz et al. (2024) conducted PMF in Fairbanks using PM<sub>1</sub> measurements with both a PTR-  
489 ToF-MS with CHARON inlet and an AMS. We focus on their PTR-ToF-MS results here since  
490 that is the same instrument used in our analysis. They found four residential heating-related factors,  
491 including three biomass burning factors and one heating oil factor, which contribute on average  
492 2.6 µg/m<sup>3</sup> (62%) of total measured OA. Although this is a much larger fraction of OA mass  
493 compared the 14% of total VOCs we attribute to residential heating, the absolute mass is much  
494 lower than our wood heating (8.6 µg/m<sup>3</sup>) and heating oil (12.1 µg/m<sup>3</sup>) factors. Ijaz et al. (2024)  
495 contribute about 1.6% (0.06 µg/m<sup>3</sup>) of measured OA to traffic, significantly less than the 29%  
496 (36.6 µg/m<sup>3</sup>) of VOCs that we contribute to the gasoline and diesel factor. They also identify a  
497 cooking factor, which we did not see resolved in our PMF analysis. This comparison shows major  
498 differences between the sources of PM<sub>1</sub> OA and gaseous VOCs. Comparison of VOC and aerosol  
499 partitioning is also explored in Ijaz et al. (2025).

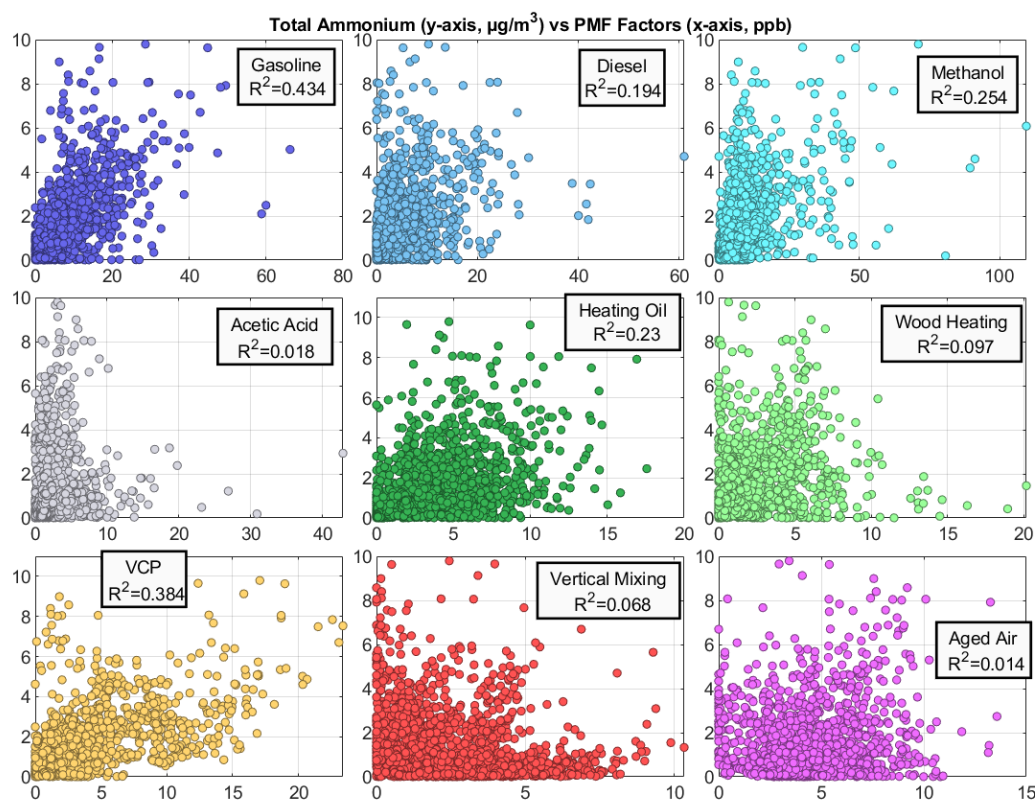
500

### 501 **3.4 PMF Comparison with Mist Chamber Total Ammonium and PILS S(IV)**

502 High concentrations of HMS and related aldehyde-S(IV) species are a unique feature of  
503 Fairbanks wintertime PM<sub>2.5</sub> (Campbell et al., 2022, 2024; Dingilian et al., 2024; Holen et al.,  
504 2025; Moon et al., 2023) and so are investigated more here. The MC-IC measures gas-phase and  
505 PM<sub>2.5</sub> aerosol-phase species. This is important for ammonium, which could have a significant  
506 portion in the gas-phase. In extremely cold environments like Fairbanks, high concentrations of  
507 total ammonium can increase aerosol pH to 4-5, greatly facilitating secondary aqueous chemistry  
508 of species like HMS and sulfate (Campbell et al., 2024). We compare MC-IC total ammonium  
509 (TA) measurements to the PMF factors in order to help determine the sources of TA.



510 Gasoline vehicles may be a large source of total ammonium in wintertime Fairbanks. We  
 511 find that TA correlates best with the gasoline factor ( $R^2 = 0.43$ ), followed by the VCP factor ( $R^2$   
 512  $= 0.38$ ) as shown in Fig. 3. TA also has a similar diurnal cycle to gasoline (Fig. S18), and is  
 513 correlated with external factors CO ( $R^2 = 0.47$ ),  $\text{NO}_x$ , ( $R^2 = 0.42$ ), and somewhat with BC ( $R^2 =$   
 514  $0.36$ ), which are commonly associated with vehicle emissions (Fig. S19). Vehicle emissions have  
 515 also been shown to be a large source of ammonia (Ji et al., 2025). Therefore, a large fraction of  
 516 TA may be coming from gasoline vehicle emissions. VCPs may also be a large source of TA, but  
 517 since VCPs include a broad category of industrial and personal care products, it is more difficult  
 518 to pinpoint exact sources.



519

520 Figure 3. Correlation of total ammonium (y-axes) with the nine PMF factors (x-axes).

521



522 HMS formation may be highly dependent on ammonia emissions (because of its effect on  
523 aerosol acidity) from gasoline vehicles and formaldehyde emissions (an HMS precursor) from  
524 diesel vehicles. PILS-IC total S(IV) correlates best with diesel ( $R^2 = 0.40$ ), followed by wood  
525 heating ( $R^2 = 0.25$ ) and gasoline ( $R^2 = 0.24$ ), as shown in Fig. S20. The total S(IV) during the  
526 ALPACA campaign was found to be mostly HMS in Dingilian et al. (2024) and Holen et al.  
527 (2025). Total S(IV) has a diurnal cycle most similar to diesel during weekdays and most similar  
528 to gasoline on the weekends (Fig. S21). Furthermore, total S(IV) has a similar diurnal cycle to  
529 formaldehyde on weekdays and  $\text{NH}_x$  on the weekends (Fig. S22). Although  $\text{SO}_2$  gas is a  
530 precursor to HMS, there are few similarities to the S(IV) and  $\text{SO}_2$  diurnal cycles (Fig. S22),  
531 which may be because  $\text{SO}_2$  gas (campaign mean 9.6 ppb) is often much higher than  
532 formaldehyde gas (campaign mean 2.3 ppb), making formaldehyde mixing ratios more often the  
533 limiting factor in HMS formation (Dingilian et al., 2024). The diesel factor is not the largest  
534 source of formaldehyde, but formation of HMS related to the gasoline and diesel factors is likely  
535 helped by both factors being emitted in the same place, and the mixing of air that occurs from  
536 moving vehicles.

537 Since the formation of HMS and other S(IV) species are secondary reactions, many other  
538 factors need to be considered, and this is not a complete picture of what drives aqueous S(IV)  
539 chemistry in Fairbanks. However, this first look seems to indicate that vehicle emissions are  
540 involved in S(IV) formation.

541

#### 542 **4. Conclusions**

543 In this work, we use online PTR-ToF-MS measurements at one minute time resolution to  
544 characterize VOCs in downtown Fairbanks during the winter 2022 ALPACA campaign. We  
545 combine these measurements with PMF analysis to examine the sources of VOCs. We further  
546 compare these sources with other complementary measurements, like total ammonium and  
547 S(IV), to help understand how VOCs can contribute to secondary aerosol formation in extremely  
548 dark and cold environments like Fairbanks.

549 High mixing ratios of many hazardous VOCs like formaldehyde, benzene, and toluene  
550 were measured in wintertime Fairbanks, with mixing ratios comparable to and often exceeding



551 measurements in other US cities. We attribute 29% of total VOC emissions to vehicle emissions  
552 and 56% to vehicle-related factors overall, with the largest factor being windshield wiper fluid.  
553 Unlike many other US cities, VCPs are a relatively minor source of VOCs. High mixing ratios of  
554 aromatics were measured and a majority of all prominent aromatic species (benzene, toluene, C8  
555 aromatics, C9 aromatics) were attributed to gasoline vehicles, followed by heating oil as the  
556 second largest aromatic factor. Sources of various carbonyls are more complex. Large portions  
557 of formaldehyde can be attributed to diesel vehicles, wood heating, vertical mixing, and possible  
558 secondary chemistry; other species like acetaldehyde and acetone can be attributed to diesel,  
559 vertical mixing, and volatile chemical products (VCPs).

560 In both our work and Ketcherside et al. (2025), a significant amount of aromatic VOCs  
561 were assigned to heating oil factors. This is in contrast to the Alaska Department of  
562 Environmental Conservation's emission inventory for ALPACA, which contributes little to no  
563 aromatic species to heating oil, as described in Zhang et al. (Zhang et al., 2026). The results of  
564 these works show a need to update the emission inventories of heating oil emission to include  
565 contributions from aromatic species.

566 We hypothesize that particulate S(IV) formation may be largely linked to vehicle  
567 emissions. Total ammonium, which allows for moderate aerosol pH in wintertime Fairbanks, is  
568 best correlated with the gasoline factor. S(IV) (largely made up of HMS) is best correlated with  
569 the diesel factor, which is the largest primary source of formaldehyde (an HMS precursor), and  
570 S(IV) has a similar diurnal cycle to both gasoline and diesel vehicles. Reductions in vehicle  
571 emissions could lead to a reduction in both harmful VOC species and secondary PM<sub>2.5</sub>  
572 formation, in Fairbanks as well as other cold and dark urban environments. This is somewhat  
573 limited by lack of ammonia measurements; simultaneous VOC, ammonia, and S(IV)  
574 measurements combined with pH modeling would help confirm these results.

575

576 **Data Availability** Meteorological data used in this study are available at  
577 <https://doi.org/10.18739/A27D2Q87W>. MC-IC, PILS-IC, and COFFEE HCHO data is available  
578 at <https://doi.org/10.18739/A2VD6P65Q>. PTR-ToF-MS data will be made available at  
579 <https://arcticdata.io/catalog/portals/ALPACA/Data> before publication.



580 **Author Contributions** SoFi PMF analysis was performed by JRC and BT-R. JRC, BT-R,  
581 B'DA, KL, RJW, KSL, MB, KKD, JM, and JM contributed to data collection and data  
582 analysis. JRC prepared the manuscript with key contributions from BT-R, BD'A, KL, JM, and  
583 contributions from all coauthors.

584

585 **Competing Interests** The authors declare that they have no conflict of interest.

586

587 **Acknowledgements** We thank William R. Simpson for measurements provided at the CTC site.

588

589 **Financial Support** The ALPACA project was initiated as a part of PACES under IGAC and  
590 with the support of IASC. J.R.C and J.M. were supported by the NSF Atmospheric and Geospace  
591 Sciences Program (grant no. AGS-2029747) and the NSF Navigating the New Arctic Program  
592 (grant no. ICER-1927750). B.D'A., K.S.L, B.T.-M. and W.Z. acknowledge support from the  
593 Agence National de Recherche (ANR) CASPA (Climate relevant Aerosol Sources and Processes  
594 in the Arctic) project (Grant ANR-21-CE010017), and the Institut polaire français Paul-Émile  
595 Victor (IPEV) (Grant 1215) and CNRS-INSU programme LEFE (Les Enveloppes Fluides et l'  
596 Environnement) ALPACA-France Projects. K.K.D., M.B. and R.J.W. were supported by the  
597 NSF Atmospheric Geoscience Program (grant no. AGS-2029730) and the NSF Navigating the  
598 New Arctic Program (grant no. ICER-1927778). M.B. acknowledges support from NASA (grant  
599 no. 80NSSC18K0557). M.C.-M was supported by the NSF Sustainably Navigating Arctic  
600 Pollution Through Engaging Communities (grant no. 1927750). J.M.S.C. acknowledges support  
601 from the NSF Atmospheric Geoscience Program (grant no. AGS-2029770).

602

603 **References**

604 Aoki, N., Inomata, S., and Tanimoto, H.: Detection of C1–C5 alkyl nitrates by proton transfer  
605 reaction time-of-flight mass spectrometry, *International Journal of Mass Spectrometry*, 263, 12–  
606 21, <https://doi.org/10.1016/j.ijms.2006.11.018>, 2007.



- 607 Baudic, A., Gros, V., Sauvage, S., Locoge, N., Sanchez, O., Sarda-Estève, R., Kalogridis, C.,  
608 Petit, J.-E., Bonnaire, N., Baisnée, D., Favez, O., Albinet, A., Sciare, J., and Bonsang, B.:  
609 Seasonal variability and source apportionment of volatile organic compounds (VOCs) in the  
610 Paris megacity (France), *Atmospheric Chemistry and Physics*, 16, 11961–11989,  
611 <https://doi.org/10.5194/acp-16-11961-2016>, 2016.
- 612 Boyce, S. D. and Hoffmann, M. R.: Kinetics and mechanism of the formation of  
613 hydroxymethanesulfonic acid at low pH, *J. Phys. Chem.*, 88, 4740–4746,  
614 <https://doi.org/10.1021/j150664a059>, 1984.
- 615 Brett, N., Law, K. S., Arnold, S. R., Fochesatto, J. G., Raut, J.-C., Onishi, T., Gilliam, R., Fahey,  
616 K., Huff, D., Pouliot, G., Barret, B., Dieudonné, E., Pohorsky, R., Schmale, J., Baccarini, A.,  
617 Bekki, S., Pappaccogli, G., Scoto, F., Decesari, S., Donato, A., Cesler-Maloney, M., Simpson,  
618 W., Medina, P., D’Anna, B., Temime-Roussel, B., Savarino, J., Albertin, S., Mao, J., Alexander,  
619 B., Moon, A., DeCarlo, P. F., Selimovic, V., Yokelson, R., and Robinson, E. S.: Investigating  
620 processes influencing simulation of local Arctic wintertime anthropogenic pollution in  
621 Fairbanks, Alaska, during ALPACA-2022, *Atmospheric Chemistry and Physics*, 25, 1063–1104,  
622 <https://doi.org/10.5194/acp-25-1063-2025>, 2025.
- 623 Campbell, J. R., Battaglia, M., Dingilian, K., Cesler-Maloney, M., St Clair, J. M., Hanisco, T. F.,  
624 Robinson, E., DeCarlo, P., Simpson, W., Nenes, A., Weber, R. J., and Mao, J.: Source and  
625 Chemistry of Hydroxymethanesulfonate (HMS) in Fairbanks, Alaska, *Environ. Sci. Technol.*,  
626 [acs.est.2c00410](https://doi.org/10.1021/acs.est.2c00410), <https://doi.org/10.1021/acs.est.2c00410>, 2022.
- 627 Campbell, J. R., Michael Battaglia Jr., Dingilian, K. K., Cesler-Maloney, M., Simpson, W. R.,  
628 Robinson, E. S., DeCarlo, P. F., Temime-Roussel, B., D’Anna, B., Holen, A. L., Wu, J., Pratt, K.  
629 A., Dibb, J. E., Nenes, A., Weber, R. J., and Mao, J.: Enhanced aqueous formation and  
630 neutralization of fine atmospheric particles driven by extreme cold, *Sci. Adv.*, 10, eado4373,  
631 <https://doi.org/10.1126/sciadv.ado4373>, 2024.
- 632 Canonaco, F., Crippa, M., Slowik, J. G., Baltensperger, U., and Prévôt, A. S. H.: SoFi, an IGOR-  
633 based interface for the efficient use of the generalized multilinear engine (ME-2) for the source  
634 apportionment: ME-2 application to aerosol mass spectrometer data, *Atmos. Meas. Tech.*, 6,  
635 3649–3661, <https://doi.org/10.5194/amt-6-3649-2013>, 2013.
- 636 Cao, Y., Zhao, H., Zhang, S., Wu, X., Anderson, J. E., Shen, W., Wallington, T. J., and Wu, Y.:  
637 Impacts of ethanol blended fuels and cold temperature on VOC emissions from gasoline vehicles  
638 in China, *Environmental Pollution*, 348, 123869, <https://doi.org/10.1016/j.envpol.2024.123869>,  
639 2024.
- 640 Cappellin, L., Karl, T., Probst, M., Ismailova, O., Winkler, P. M., Soukoulis, C., Aprea, E.,  
641 Märk, T. D., Gasperi, F., and Biasioli, F.: On Quantitative Determination of Volatile Organic  
642 Compound Concentrations Using Proton Transfer Reaction Time-of-Flight Mass Spectrometry,  
643 *Environ. Sci. Technol.*, 46, 2283–2290, <https://doi.org/10.1021/es203985t>, 2012.
- 644 Cesler-Maloney, M., Simpson, W. R., Miles, T., Mao, J., Law, K. S., and Roberts, T. J.:  
645 Differences in Ozone and Particulate Matter Between Ground Level and 20 m Aloft are Frequent  
646 During Wintertime Surface-Based Temperature Inversions in Fairbanks, Alaska, *Journal of*



- 647 Geophysical Research: Atmospheres, 127, e2021JD036215,  
648 <https://doi.org/10.1029/2021JD036215>, 2022.
- 649 Cofer, W. R., Collins, V. G., and Talbot, R. W.: Improved aqueous scrubber for collection of  
650 soluble atmospheric trace gases, *Environ. Sci. Technol.*, 19, 557–560,  
651 <https://doi.org/10.1021/es00136a012>, 1985.
- 652 Coggon, M. M., Lim, C. Y., Koss, A. R., Sekimoto, K., Yuan, B., Gilman, J. B., Hagan, D. H.,  
653 Selimovic, V., Zarzana, K. J., Brown, S. S., Roberts, J. M., Müller, M., Yokelson, R., Wisthaler,  
654 A., Krechmer, J. E., Jimenez, J. L., Cappa, C., Kroll, J. H., de Gouw, J., and Warneke, C.: OH  
655 chemistry of non-methane organic gases (NMOGs) emitted from laboratory and ambient  
656 biomass burning smoke: evaluating the influence of furans and oxygenated aromatics on ozone  
657 and secondary NMOG formation, *Atmospheric Chemistry and Physics*, 19, 14875–14899,  
658 <https://doi.org/10.5194/acp-19-14875-2019>, 2019.
- 659 Coggon, M. M., Stockwell, C. E., Clafin, M. S., Pfannerstill, E. Y., Xu, L., Gilman, J. B.,  
660 Marcantonio, J., Cao, C., Bates, K., Gkatzelis, G. I., Lamplugh, A., Katz, E. F., Arata, C., Apel,  
661 E. C., Hornbrook, R. S., Piel, F., Majluf, F., Blake, D. R., Wisthaler, A., Canagaratna, M.,  
662 Lerner, B. M., Goldstein, A. H., Mak, J. E., and Warneke, C.: Identifying and correcting  
663 interferences to PTR-ToF-MS measurements of isoprene and other urban volatile organic  
664 compounds, *Atmospheric Measurement Techniques*, 17, 801–825, [https://doi.org/10.5194/amt-](https://doi.org/10.5194/amt-17-801-2024)  
665 [17-801-2024](https://doi.org/10.5194/amt-17-801-2024), 2024.
- 666 Dingilian, K., Hebert, E., Battaglia, M. Jr., Campbell, J. R., Cesler-Maloney, M., Simpson, W.,  
667 St. Clair, J. M., Dibb, J., Temime-Roussel, B., D’Anna, B., Moon, A., Alexander, B., Yang, Y.,  
668 Nenes, A., Mao, J., and Weber, R. J.: Hydroxymethanesulfonate and Sulfur(IV) in Fairbanks  
669 Winter During the ALPACA Study, *ACS EST Air*, <https://doi.org/10.1021/acsestair.4c00012>,  
670 2024.
- 671 Eliason, T. L., Aloisio, S., Donaldson, D. J., Cziczo, D. J., and Vaida, V.: Processing of  
672 unsaturated organic acid films and aerosols by ozone, *Atmospheric Environment*, 37, 2207–  
673 2219, [https://doi.org/10.1016/S1352-2310\(03\)00149-3](https://doi.org/10.1016/S1352-2310(03)00149-3), 2003.
- 674 Ferrarese, C., Franzetti, J., Selleri, T., and Suarez-Bertoa, R.: VOC emissions from Euro 6  
675 vehicles, *Environ Sci Eur*, 36, 27, <https://doi.org/10.1186/s12302-024-00854-4>, 2024.
- 676 George, I. J., Hays, M. D., Herrington, J. S., Preston, W., Snow, R., Faircloth, J., George, B. J.,  
677 Long, T., and Baldauf, R. W.: Effects of Cold Temperature and Ethanol Content on VOC  
678 Emissions from Light-Duty Gasoline Vehicles, *Environ. Sci. Technol.*, 49, 13067–13074,  
679 <https://doi.org/10.1021/acs.est.5b04102>, 2015.
- 680 Gkatzelis, G. I., Coggon, M. M., McDonald, B. C., Peischl, J., Gilman, J. B., Aikin, K. C.,  
681 Robinson, M. A., Canonaco, F., Prevot, A. S. H., Trainer, M., and Warneke, C.: Observations  
682 Confirm that Volatile Chemical Products Are a Major Source of Petrochemical Emissions in  
683 U.S. Cities, *Environ. Sci. Technol.*, 55, 4332–4343, <https://doi.org/10.1021/acs.est.0c05471>,  
684 2021.



- 685 de Gouw, J. and Warneke, C.: Measurements of volatile organic compounds in the earth's  
686 atmosphere using proton-transfer-reaction mass spectrometry, *Mass Spectrometry Reviews*, 26,  
687 223–257, <https://doi.org/10.1002/mas.20119>, 2007.
- 688 Grosjean, D., Swanson, R. D., and Ellis, C.: Carbonyls in Los Angeles air: Contribution of direct  
689 emissions and photochemistry, *Science of The Total Environment*, 29, 65–85,  
690 [https://doi.org/10.1016/0048-9697\(83\)90034-7](https://doi.org/10.1016/0048-9697(83)90034-7), 1983.
- 691 Gueneron, M., Erickson, M. H., VanderSchelden, G. S., and Jobson, B. T.: PTR-MS  
692 fragmentation patterns of gasoline hydrocarbons, *International Journal of Mass Spectrometry*,  
693 379, 97–109, <https://doi.org/10.1016/j.ijms.2015.01.001>, 2015.
- 694 Guenther, A., Hewitt, C. N., Erickson, D., Fall, R., Geron, C., Graedel, T., Harley, P., Klinger,  
695 L., Lerdau, M., Mckay, W. A., Pierce, T., Scholes, B., Steinbrecher, R., Tallamraju, R., Taylor,  
696 J., and Zimmerman, P.: A global model of natural volatile organic compound emissions, *Journal*  
697 *of Geophysical Research: Atmospheres*, 100, 8873–8892, <https://doi.org/10.1029/94JD02950>,  
698 1995.
- 699 Hansel, A. and Wisthaler, A.: A method for real-time detection of PAN, PPN and MPAN in  
700 ambient air, *Geophysical Research Letters*, 27, 895–898, <https://doi.org/10.1029/1999GL010989>,  
701 2000.
- 702 Hays, M. D., Preston, W., George, B. J., George, I. J., Snow, R., Faircloth, J., Long, T., Baldauf,  
703 R. W., and McDonald, J.: Temperature and Driving Cycle Significantly Affect Carbonaceous  
704 Gas and Particle Matter Emissions from Diesel Trucks, *Energy Fuels*, 31, 11034–11042,  
705 <https://doi.org/10.1021/acs.energyfuels.7b01446>, 2017.
- 706 Heald, C. L., Goldstein, A. H., Allan, J. D., Aiken, A. C., Apel, E., Atlas, E. L., Baker, A. K.,  
707 Bates, T. S., Beyersdorf, A. J., Blake, D. R., Campos, T., Coe, H., Crounse, J. D., DeCarlo, P. F.,  
708 de Gouw, J. A., Dunlea, E. J., Flocke, F. M., Fried, A., Goldan, P., Griffin, R. J., Herndon, S. C.,  
709 Holloway, J. S., Holzinger, R., Jimenez, J. L., Junkermann, W., Kuster, W. C., Lewis, A. C.,  
710 Meinardi, S., Millet, D. B., Onasch, T., Polidori, A., Quinn, P. K., Riemer, D. D., Roberts, J. M.,  
711 Salcedo, D., Sive, B., Swanson, A. L., Talbot, R., Warneke, C., Weber, R. J., Weibring, P.,  
712 Wennberg, P. O., Worsnop, D. R., Wittig, A. E., Zhang, R., Zheng, J., and Zheng, W.: Total  
713 observed organic carbon (TOOC) in the atmosphere: a synthesis of North American  
714 observations, *Atmospheric Chemistry and Physics*, 8, 2007–2025, [https://doi.org/10.5194/acp-8-](https://doi.org/10.5194/acp-8-2007-2008)  
715 2007-2008, 2008.
- 716 Heald, C. L., Gouw, J. de, Goldstein, A. H., Guenther, A. B., Hayes, P. L., Hu, W., Isaacman-  
717 VanWertz, G., Jimenez, J. L., Keutsch, F. N., Koss, A. R., Misztal, P. K., Rappenglück, B.,  
718 Roberts, J. M., Stevens, P. S., Washenfelder, R. A., Warneke, C., and Young, C. J.: Contrasting  
719 Reactive Organic Carbon Observations in the Southeast United States (SOAS) and Southern  
720 California (CalNex), *Environ. Sci. Technol.*, 54, 14923–14935,  
721 <https://doi.org/10.1021/acs.est.0c05027>, 2020.
- 722 Holen, A. L., Wu, J., Forshee, L., Dingilian, K. K., Selimovic, V., Battaglia, M. A., Robinson, E.  
723 S., Cysneiros De Carvalho, K., Ketcherside, D. T., Campbell, J. R., Moon, A., Alexander, B.,  
724 Simpson, W. R., Mao, J., Hu, L., Williams, B. J., DeCarlo, P. F., Weber, R. J., and Pratt, K. A.:



- 725 Quantifying Contributions of Sulfate, Hydroxymethanesulfonate, and Additional S(IV)  
726 Compounds to Wintertime Aerosol Particles, ACS EST Air, acsestair.5c00232,  
727 <https://doi.org/10.1021/acsestair.5c00232>, 2025.
- 728 Huang, W., Yu, X., Deng, H., Chen, B., Cheng, P., Yang, W., Li, M., Yuan, B., Wang, M., and  
729 Gong, Y.: Strong Seasonal Transition and Complex Sources of Volatile Organic Compounds at  
730 an Urban Site in Guangzhou, China, *Journal of Geophysical Research: Atmospheres*, 129,  
731 e2024JD040890, <https://doi.org/10.1029/2024JD040890>, 2024.
- 732 Ijaz, A., Temime-Roussel, B., Chazeau, B., Albertin, S., Arnold, S. R., Barrett, B., Bekki, S.,  
733 Brett, N., Cesler-Maloney, M., Dieudonne, E., Dingilian, K. K., Fochesatto, J. G., Mao, J.,  
734 Moon, A., Savarino, J., Simpson, W., Weber, R. J., Law, K. S., and D'Anna, B.: Complementary  
735 aerosol mass spectrometry elucidates sources of wintertime sub-micron particle pollution in  
736 Fairbanks, Alaska, during ALPACA 2022, <https://doi.org/10.5194/egusphere-2024-3789>, 12  
737 December 2024.
- 738 Ijaz, A., Temime-Roussel, B., Kammer, J., Mao, J., Simpson, W., Law, K. S., and D'Anna, B.:  
739 *In situ* measurements of gas–particle partitioning of organic compounds in Fairbanks, *Faraday*  
740 *Discuss.*, 10.1039.D4FD00175C, <https://doi.org/10.1039/D4FD00175C>, 2025.
- 741 Ji, Z., Bao, Z., Chen, H., Zhang, P., Luo, D., Wu, H., Geng, L., Cao, J., and Yan, X.: Overview  
742 of the Generation Mechanism, Influence Factors, and Control Technologies of NH<sub>3</sub> Emissions  
743 from Road Transport Vehicles, *Environ. Sci. Technol.*, <https://doi.org/10.1021/acs.est.5c11764>,  
744 2025.
- 745 Ketcherside, D., Yokelson, R. J., Selimovic, V., Robinson, E. S., Cesler-Maloney, M., Holen, A.  
746 L., Wu, J., Temime-Roussel, B., Ijaz, A., Kuhn, J., Moon, A., Pappaccogli, G., Carvalho, K. C.  
747 D., Decesari, S., Alexander, B., Williams, B. J., D'Anna, B., Stutz, J., Pratt, K. A., DeCarlo, P.  
748 F., Mao, J., Simpson, W. R., Hopke, P. K., and Hu, L.: Wintertime Abundance and Sources of  
749 Key Trace Gas and Particle Species in Fairbanks, Alaska,  
750 <https://doi.org/10.22541/essoar.174139360.08941913/v1>, 8 March 2025.
- 751 Kossover, R.: Association between Air Quality and Hospital Visits — Fairbanks, 2003–2008,  
752 2010.
- 753 Kotchenruther, R. A.: Source apportionment of PM 2.5 at multiple Northwest U.S. sites:  
754 Assessing regional winter wood smoke impacts from residential wood combustion, *Atmospheric*  
755 *Environment*, 142, 210–219, <https://doi.org/10.1016/j.atmosenv.2016.07.048>, 2016.
- 756 Languille, B., Gros, V., Petit, J.-E., Honoré, C., Baudic, A., Perrussel, O., Foret, G., Michoud,  
757 V., Truong, F., Bonnaire, N., Sarda-Estève, R., Delmotte, M., Feron, A., Maisonneuve, F.,  
758 Gaimoz, C., Formenti, P., Kotthaus, S., Haeffelin, M., and Favez, O.: Wood burning: A major  
759 source of Volatile Organic Compounds during wintertime in the Paris region, *Science of The*  
760 *Total Environment*, 711, 135055, <https://doi.org/10.1016/j.scitotenv.2019.135055>, 2020.
- 761 Lannuque, V., D'Anna, B., Kostenidou, E., Couvidat, F., Martinez-Valiente, A., Eichler, P.,  
762 Wisthaler, A., Müller, M., Temime-Roussel, B., Valorso, R., and Sartelet, K.: Gas–particle



- 763 partitioning of toluene oxidation products: an experimental and modeling study, *Atmos. Chem.*  
764 *Phys.*, 23, 15537–15560, <https://doi.org/10.5194/acp-23-15537-2023>, 2023.
- 765 Legreid, G., Lööv, J. B., Staehelin, J., Hueglin, C., Hill, M., Buchmann, B., Prevot, A. S. H., and  
766 Reimann, S.: Oxygenated volatile organic compounds (OVOCs) at an urban background site in  
767 Zürich (Europe): Seasonal variation and source allocation, *Atmospheric Environment*, 41, 8409–  
768 8423, <https://doi.org/10.1016/j.atmosenv.2007.07.026>, 2007.
- 769 Li, J., Xie, S. D., Zeng, L. M., Li, L. Y., Li, Y. Q., and Wu, R. R.: Characterization of ambient  
770 volatile organic compounds and their sources in Beijing, before, during, and after Asia-Pacific  
771 Economic Cooperation China 2014, *Atmospheric Chemistry and Physics*, 15, 7945–7959,  
772 <https://doi.org/10.5194/acp-15-7945-2015>, 2015.
- 773 Li, K., Li, J., Tong, S., Wang, W., Huang, R.-J., and Ge, M.: Characteristics of wintertime VOCs  
774 in suburban and urban Beijing: concentrations, emission ratios, and festival effects, *Atmospheric*  
775 *Chemistry and Physics*, 19, 8021–8036, <https://doi.org/10.5194/acp-19-8021-2019>, 2019.
- 776 Li, S., Liu, D., Wu, Y., Hu, K., Jiang, X., Tian, P., Sheng, J., Pan, B., and Zhao, D.: Aging  
777 effects on residential biomass burning emissions under quasi-real atmospheric conditions,  
778 *Environmental Pollution*, 337, 122615, <https://doi.org/10.1016/j.envpol.2023.122615>, 2023.
- 779 Liu, X., Wang, Y., Zhu, R., Wei, Y., and Hu, J.: Complex temperature dependence of vehicular  
780 emissions: Evidence from a global meta-analysis, *Environmental Research*, 237, 116890,  
781 <https://doi.org/10.1016/j.envres.2023.116890>, 2023.
- 782 Marques, B., Kostenidou, E., Valiente, A. M., Vansevenant, B., Sarica, T., Fine, L., Temime-  
783 Roussel, B., Tassel, P., Perret, P., Liu, Y., Sartelet, K., Ferronato, C., and D’Anna, B.: Detailed  
784 Speciation of Non-Methane Volatile Organic Compounds in Exhaust Emissions from Diesel and  
785 Gasoline Euro 5 Vehicles Using Online and Offline Measurements, *Toxics*, 10, 184,  
786 <https://doi.org/10.3390/toxics10040184>, 2022.
- 787 McDonald, B. C., De Gouw, J. A., Gilman, J. B., Jathar, S. H., Akherati, A., Cappa, C. D.,  
788 Jimenez, J. L., Lee-Taylor, J., Hayes, P. L., McKeen, S. A., Cui, Y. Y., Kim, S.-W., Gentner, D.  
789 R., Isaacman-VanWertz, G., Goldstein, A. H., Harley, R. A., Frost, G. J., Roberts, J. M.,  
790 Ryerson, T. B., and Trainer, M.: Volatile chemical products emerging as largest petrochemical  
791 source of urban organic emissions, *Science*, 359, 760–764,  
792 <https://doi.org/10.1126/science.aq0524>, 2018.
- 793 Mehra, A., Wang, Y., Krechmer, J. E., Lambe, A., Majluf, F., Morris, M. A., Priestley, M.,  
794 Bannan, T. J., Bryant, D. J., Pereira, K. L., Hamilton, J. F., Rickard, A. R., Newland, M. J.,  
795 Stark, H., Croteau, P., Jayne, J. T., Worsnop, D. R., Canagaratna, M. R., Wang, L., and Coe, H.:  
796 Evaluation of the chemical composition of gas- and particle-phase products of aromatic  
797 oxidation, *Atmos. Chem. Phys.*, 20, 9783–9803, <https://doi.org/10.5194/acp-20-9783-2020>,  
798 2020.
- 799 Millet, D. B., Donahue, N. M., Pandis, S. N., Polidori, A., Stanier, C. O., Turpin, B. J., and  
800 Goldstein, A. H.: Atmospheric volatile organic compound measurements during the Pittsburgh  
801 Air Quality Study: Results, interpretation, and quantification of primary and secondary



- 802 contributions, *Journal of Geophysical Research: Atmospheres*, 110,  
803 <https://doi.org/10.1029/2004JD004601>, 2005.
- 804 Moon, A., Jongebloed, U., Dingilian, K. K., Schauer, A. J., Chan, Y.-C., Cesler-Maloney, M.,  
805 Simpson, W. R., Weber, R. J., Tsiang, L., Yazbeck, F., Zhai, S., Wedum, A., Turner, A. J.,  
806 Albertin, S., Bekki, S., Savarino, J., Gribanov, K., Pratt, K. A., Costa, E. J., Anastasio, C.,  
807 Sunday, M. O., Heinlein, L. M. D., Mao, J., and Alexander, B.: Primary Sulfate Is the Dominant  
808 Source of Particulate Sulfate during Winter in Fairbanks, Alaska, *ACS EST Air*,  
809 <https://doi.org/10.1021/acsestair.3c00023>, 2023.
- 810 Nattinger, K. C.: TEMPORAL AND SPATIAL TRENDS OF FINE PARTICULATE MATTER  
811 COMPOSITION IN FAIRBANKS, ALASKA, 2016.
- 812 Norris, G., Duvall, R., Brown, S., and Bai, S.: Positive Matrix Factorization (PMF) 5.0  
813 Fundamentals and User Guide, 2014.
- 814 Nuvolone, D., Petri, D., and Voller, F.: The effects of ozone on human health, *Environ Sci Pollut*  
815 *Res*, 25, 8074–8088, <https://doi.org/10.1007/s11356-017-9239-3>, 2018.
- 816 Orsini, D. A., Ma, Y., Sullivan, A., Sierau, B., Baumann, K., and Weber, R. J.: Refinements to  
817 the particle-into-liquid sampler (PILS) for ground and airborne measurements of water soluble  
818 aerosol composition, *Atmospheric Environment*, 37, 1243–1259,  
819 [http://dx.doi.org/10.1016/S1352-2310\(02\)01015-4](http://dx.doi.org/10.1016/S1352-2310(02)01015-4), 2003.
- 820 Paatero, P.: The Multilinear Engine: A Table-Driven, Least Squares Program for Solving  
821 Multilinear Problems, including the n-Way Parallel Factor Analysis Model, *Journal of*  
822 *Computational and Graphical Statistics*, 8, 854–888, <https://doi.org/10.2307/1390831>, 1999.
- 823 Paatero, P. and Hopke, P. K.: Discarding or downweighting high-noise variables in factor  
824 analytic models, *Analytica Chimica Acta*, 490, 277–289, [https://doi.org/10.1016/S0003-](https://doi.org/10.1016/S0003-2670(02)01643-4)  
825 [2670\(02\)01643-4](https://doi.org/10.1016/S0003-2670(02)01643-4), 2003.
- 826 Patokoski, J., Ruuskanen, T. M., Hellén, H., Taipale, R., Grönholm, T., Kajos, M. K., Petäjä, T.,  
827 Hakola, H., Kulmala, M., and Rinne, J.: Winter to spring transition and diurnal variation of  
828 VOCs in Finland at an urban background site and a rural site, 19, 2014.
- 829 Paulot, F., Wunch, D., Crouse, J. D., Toon, G. C., Millet, D. B., DeCarlo, P. F., Vigouroux, C.,  
830 Deutscher, N. M., González Abad, G., Notholt, J., Warneke, T., Hannigan, J. W., Warneke, C.,  
831 de Gouw, J. A., Dunlea, E. J., De Mazière, M., Griffith, D. W. T., Bernath, P., Jimenez, J. L., and  
832 Wennberg, P. O.: Importance of secondary sources in the atmospheric budgets of formic and  
833 acetic acids, *Atmospheric Chemistry and Physics*, 11, 1989–2013, [https://doi.org/10.5194/acp-](https://doi.org/10.5194/acp-11-1989-2011)  
834 [11-1989-2011](https://doi.org/10.5194/acp-11-1989-2011), 2011.
- 835 Pope III, C. A. and Dockery, D. W.: Health Effects of Fine Particulate Air Pollution: Lines that  
836 Connect, *Journal of the Air & Waste Management Association*, 56, 709–742,  
837 <https://doi.org/10.1080/10473289.2006.10464485>, 2006.



- 838 Rao, Z., Chen, Z., Liang, H., Huang, L., and Huang, D.: Carbonyl compounds over urban  
839 Beijing: Concentrations on haze and non-haze days and effects on radical chemistry,  
840 *Atmospheric Environment*, 124, 207–216, <https://doi.org/10.1016/j.atmosenv.2015.06.050>, 2016.
- 841 Rivellini, L.-H., Jorga, S., Wang, Y., Lee, A. K. Y., Murphy, J. G., Chan, A. W., and Abbatt, J.  
842 P. D.: Sources of Wintertime Atmospheric Organic Pollutants in a Large Canadian City: Insights  
843 from Particle and Gas Phase Measurements, *ACS EST Air*, 1, 690–703,  
844 <https://doi.org/10.1021/acsestair.4c00039>, 2024.
- 845 Sadeghi, B., Pouyaei, A., Choi, Y., and Rappenglueck, B.: Influence of seasonal variability on  
846 source characteristics of VOCs at Houston industrial area, *Atmospheric Environment*, 277,  
847 119077, <https://doi.org/10.1016/j.atmosenv.2022.119077>, 2022.
- 848 Schwartz, J., Laden, F., and Zanobetti, A.: The concentration-response relation between PM(2.5)  
849 and daily deaths., *Environ Health Perspect*, 110, 1025–1029,  
850 <https://doi.org/10.1289/ehp.021101025>, 2002.
- 851 Seinfeld, J. H. and Pandis, S. N.: *Atmospheric Chemistry and Physics: From Air Pollution to*  
852 *Climate Change*, John Wiley & Sons, Hoboken, 2016.
- 853 Sharma, N., Agarwal, A. K., Eastwood, P., Gupta, T., and Singh, A. P. (Eds.): *Air Pollution and*  
854 *Control*, Springer Singapore, Singapore, <https://doi.org/10.1007/978-981-10-7185-0>, 2018.
- 855 Simpson, W. R., Mao, J., Fochesatto, G. J., Law, K. S., DeCarlo, P. F., Schmale, J., Pratt, K. A.,  
856 Arnold, S. R., Stutz, J., Dibb, J. E., Creamean, J. M., Weber, R. J., Williams, B. J., Alexander,  
857 B., Hu, L., Yokelson, R. J., Shiraiwa, M., Decesari, S., Anastasio, C., D’Anna, B., Gilliam, R.  
858 C., Nenes, A., St. Clair, J. M., Trost, B., Flynn, J. H., Savarino, J., Conner, L. D., Kettle, N.,  
859 Heeringa, K. M., Albertin, S., Baccarini, A., Barret, B., Battaglia, M. A., Bekki, S., Brado, T. J.,  
860 Brett, N., Brus, D., Campbell, J. R., Cesler-Maloney, M., Cooperdock, S., Cysneiros de  
861 Carvalho, K., Delbarre, H., DeMott, P. J., Dennehy, C. J. S., Dieudonné, E., Dingilian, K. K.,  
862 Donato, A., Douglgeris, K. M., Edwards, K. C., Fahey, K., Fang, T., Guo, F., Heinlein, L. M. D.,  
863 Holen, A. L., Huff, D., Ijaz, A., Johnson, S., Kapur, S., Ketcherside, D. T., Levin, E., Lill, E.,  
864 Moon, A. R., Onishi, T., Pappaccogli, G., Perkins, R., Pohorsky, R., Raut, J.-C., Ravetta, F.,  
865 Roberts, T., Robinson, E. S., Scotto, F., Selimovic, V., Sunday, M. O., Temime-Roussel, B.,  
866 Tian, X., Wu, J., and Yang, Y.: Overview of the Alaskan Layered Pollution and Chemical  
867 Analysis (ALPACA) Field Experiment, *ACS EST Air*, 1, 200–222,  
868 <https://doi.org/10.1021/acsestair.3c00076>, 2024.
- 869 Slowik, J. G., Vlasenko, A., McGuire, M., Evans, G. J., and Abbatt, J. P. D.: Simultaneous factor  
870 analysis of organic particle and gas mass spectra: AMS and PTR-MS measurements at an urban  
871 site, *Atmospheric Chemistry and Physics*, 10, 1969–1988, [https://doi.org/10.5194/acp-10-1969-](https://doi.org/10.5194/acp-10-1969-2010)  
872 2010, 2010.
- 873 Song, S., Gao, M., Xu, W., Sun, Y., Worsnop, D. R., Jayne, J. T., Zhang, Y., Zhu, L., Li, M.,  
874 Zhou, Z., Cheng, C., Lv, Y., Wang, Y., Peng, W., Xu, X., Lin, N., Wang, Y., Wang, S., Munger,  
875 J. W., Jacob, D. J., and McElroy, M. B.: Possible heterogeneous chemistry of  
876 hydroxymethanesulfonate (HMS) in northern China winter haze, *Atmos. Chem. Phys.*, 19, 1357–  
877 1371, <https://doi.org/10.5194/acp-19-1357-2019>, 2019.



- 878 St. Clair, J. M., Swanson, A. K., Bailey, S. A., Wolfe, G. M., Marrero, J. E., Iraci, L. T.,  
879 Hagopian, J. G., and Hanisco, T. F.: A new non-resonant laser-induced fluorescence instrument  
880 for the airborne in situ measurement of formaldehyde, *Atmospheric Measurement Techniques*,  
881 10, 4833–4844, <https://doi.org/10.5194/amt-10-4833-2017>, 2017.
- 882 Suarez-Bertoa, R., Selleri, T., Gioria, R., Melas, A. D., Ferrarese, C., Franzetti, J., Arlitt, B.,  
883 Nagura, N., Hanada, T., and Giechaskiel, B.: Real-Time Measurements of Formaldehyde  
884 Emissions from Modern Vehicles, *Energies*, 15, 7680, <https://doi.org/10.3390/en15207680>,  
885 2022.
- 886 Vlasenko, A., Macdonald, A. M., Sjostedt, S. J., and Abbatt, J. P. D.: Formaldehyde  
887 measurements by Proton transfer reaction – Mass Spectrometry (PTR-MS): correction for  
888 humidity effects, *Atmospheric Measurement Techniques*, 3, 1055–1062,  
889 <https://doi.org/10.5194/amt-3-1055-2010>, 2010.
- 890 Wærsted, E. G., Sundvor, I., Denby, B. R., and Mu, Q.: Quantification of temperature  
891 dependence of NO emissions from road traffic in Norway using air quality modelling and  
892 monitoring data, *Atmospheric Environment: X*, 13, 100160,  
893 <https://doi.org/10.1016/j.aeaoa.2022.100160>, 2022.
- 894 Wang, L., Slowik, J. G., Tripathi, N., Bhattu, D., Rai, P., Kumar, V., Vats, P., Satish, R.,  
895 Baltensperger, U., Ganguly, D., Rastogi, N., Sahu, L. K., Tripathi, S. N., and Prévôt, A. S. H.:  
896 Source characterization of volatile organic compounds measured by proton-transfer-reaction  
897 time-of-flight mass spectrometers in Delhi, India, *Atmospheric Chemistry and Physics*, 20,  
898 9753–9770, <https://doi.org/10.5194/acp-20-9753-2020>, 2020.
- 899 Wang, L., Slowik, J. G., Tong, Y., Duan, J., Gu, Y., Rai, P., Qi, L., Stefenelli, G., Baltensperger,  
900 U., Huang, R.-J., Cao, J., and Prévôt, A. S. H.: Characteristics of wintertime VOCs in urban  
901 Beijing: Composition and source apportionment, *Atmospheric Environment: X*, 9, 100100,  
902 <https://doi.org/10.1016/j.aeaoa.2020.100100>, 2021.
- 903 Wang, L., Slowik, J. G., Klein, F., Stefenelli, G., Pospisilova, V., Tong, Y., Baltensperger, U.,  
904 and Prévôt, A. S. H.: Characteristics of oxygenated volatile organic compounds in Zurich,  
905 Switzerland: Sources, composition, and implication for secondary aerosol formation,  
906 *Chemosphere*, 368, 143686, <https://doi.org/10.1016/j.chemosphere.2024.143686>, 2024.
- 907 Wang, S., Yuan, B., Wu, C., Wang, C., Li, T., He, X., Huangfu, Y., Qi, J., Li, X.-B., Sha, Q.,  
908 Zhu, M., Lou, S., Wang, H., Karl, T., Graus, M., Yuan, Z., and Shao, M.: Oxygenated volatile  
909 organic compounds (VOCs) as significant but varied contributors to VOC emissions from  
910 vehicles, *Atmos. Chem. Phys.*, 22, 9703–9720, <https://doi.org/10.5194/acp-22-9703-2022>, 2022.
- 911 Ward, T., Trost, B., Conner, J., Flanagan, J., and Jayanty, R. K. M.: Source Apportionment of  
912 PM<sub>2.5</sub> in a Subarctic Airshed - Fairbanks, Alaska, *Aerosol Air Qual. Res.*, 12, 536–543,  
913 <https://doi.org/10.4209/aaqr.2011.11.0208>, 2012.
- 914 Yano, Y., Morris, S. S., Salerno, C., Schlapia, A. M., and Stichick, M.: Impact of a new gasoline  
915 benzene regulation on ambient air pollutants in Anchorage, Alaska, *Atmospheric Environment*,  
916 132, 276–282, <https://doi.org/10.1016/j.atmosenv.2016.02.039>, 2016.



917 Zhang, W., Brett, N., Law, K. S., Temime-Roussel, B., D'Anna, B., Onishi, T., Raut, J.-C.,  
918 Bekki, S., Barret, B., Arnold, S. R., Savarino, J., Yokelson, R. J., Hu, L., Huff, D., Mao, J.,  
919 Campbell, J., Pappaccogli, G., Pohorsky, R., Schmale, J., and Simpson, W. R.: Exploring factors  
920 influencing sources and distributions of aromatics in an Arctic winter urban environment, in  
921 press, 2026.

922 Zhou, L., Xiong, Y., Sera, F., Vicedo-Cabrera, A. M., Abrutzky, R., Guo, Y., Tong, S., Coelho,  
923 M. de S. Z. S., Saldiva, P. H. N., Lavigne, E., Correa, P. M., Ortega, N. V., Osorio, S., Roye, D.,  
924 Kyselý, J., Orru, H., Maasikmets, M., Jaakkola, J. J. K., Rytí, N., Pascal, M., Huber, V.,  
925 Breitner-Busch, S., Schneider, A., Katsouyanni, K., Samoli, E., Entezari, A., Mayvaneh, F.,  
926 Goodman, P., Zeka, A., Raz, R., Scortichini, M., Stafoggia, M., Honda, Y., Hashizume, M., Ng,  
927 C. F. S., Alahmad, B., Diaz, M. H., Arellano, E. E. F., Overcenco, A., Klompmaker, J., Rao, S.,  
928 Carrasco, G., Seposo, X., Chua, P. L. C., Silva, S. das N. P. da, Madureira, J., Holobaca, I.-H.,  
929 Scovronick, N., Garland, R. M., Kim, H., Lee, W., Tobias, A., Íñiguez, C., Forsberg, B., Ragetti,  
930 M. S., Guo, Y. L., Pan, S.-C., Li, S., Masselot, P., Colistro, V., Bell, M., Zanobetti, A., Schwartz,  
931 J., Dang, T. N., Dung, D. V., Gasparrini, A., Huang, Y., and Kan, H.: Associations of ambient  
932 exposure to benzene, toluene, ethylbenzene, and xylene with daily mortality: a multicountry  
933 time-series study in 757 global locations, *The Lancet Planetary Health*, 9,  
934 <https://doi.org/10.1016/j.lanplh.2025.101306>, 2025.

935 Ziemann, P. J. and Atkinson, R.: Kinetics, products, and mechanisms of secondary organic  
936 aerosol formation, *Chem. Soc. Rev.*, 41, 6582, <https://doi.org/10.1039/c2cs35122f>, 2012.

937